PHILOSOPHICAL TRANSACTIONS OF THE ROYAL SOCIETY A MATHEMATICAL, PHYSICAL & ENGINEERING SCIENCES

Magnetic anisotropy in molecule–based magnets

Olivier Kahn

Phil. Trans. R. Soc. Lond. A 1999 **357**, 3005-3023
doi: 10.1098/rsta.1999.0478

Magnetic anisotropy in molecule-based magnets

By Olivier Kahn

Laboratoire des Sciences Moléculaires, Institut de Chimie de la Matière Condensée de Bordeaux, UPR CNRS No. 9048, 33608 Pessac, France

The goal of this paper is to introduce the dimension 'magnetic anisotropy' in the field of molecule-based magnets. For that, we have focused on two aspects, namely the design of a hard magnet through the incorporation of magnetically anisotropic spin carriers, and the determination of the magnetic phase diagrams of two strongly anisotropic ferromagnets. The hard magnet contains three kinds of spin carriers, Co^{II} and Cu^{II} ions as well as radical cations. It structure is very peculiar; it consists of two perpendicular honeycomb-like networks which interpenetrate in such a way that each hexagon belonging to one of the networks is interlocked with a hexagon belonging to the perpendicular network. The coercive field depends on the grain size. It can be as large as 25 kOe at 5 K. The two strongly anisotropic ferromagnets are cyano-bridged $Mn^{II}Mo^{III}$ compounds synthesized from the $[Mo^{III}(CN)_7]^{4-}$ precursor. Mo^{III} has a low-spin configuration, with a local spin $S_{Mo} = 1/2$, and a strongly anisotropic $\boldsymbol{g}$ tensor. One of the compounds, $Mn_2(H_2O)_5Mo(CN)_7 \cdot 4H_2O$, has a three-dimensional structure. The other one, $K_2Mn_3(H_2O)_6[Mo(CN)_7]_2 \cdot 6H_2O$, has a two-dimensional structure. For both compounds, we have succeeded to grow well-shaped single crystals suitable for magnetic anisotropy measurements, and we have investigated the magnetic properties as follows: first, we have determined the magnetic axes by looking for the extremes of the magnetization in the three crystallographic planes, *ab*, *bc*, and *ac*. Then, we have measured the temperature and field dependencies of the magnetization in the DC mode along the three magnetic axes. These measurements have revealed the existence of several magnetically ordered phases for the three-dimensional compound, and of field-induced spin reorientations for both compounds. For the very first time in the field of molecular magnetism, we believe we have been able to determine the magnetic phase diagrams.

Keywords: coercivity; magnetic anisotropy; magnetic phase diagrams; molecule-based magnet; molecular material; supramolecular chemistry

1. Introduction

The first two molecular compounds exhibiting a spontaneous magnetization below a certain critical temperature, T_c, were described in 1986 (Miller *et al.* 1986; Pei *et al.* 1986). These reports have opened a new field of research, that of molecule-based magnets, and in the last decade quite a few new compounds of that kind have been synthesized (Miller *et al.* 1987; Kahn *et al.* 1988; Caneschi *et al.* 1989; Broderick *et al.* 1990; Yee *et al.* 1991; Nakazawa *et al.* 1992; Tamaki *et al.* 1992; Chiarelli *et al.* 1993; Miller & Epstein 1994; Gatteschi 1994; Inoue & Iwamura 1994; Decurtins *et al.* 1994*a*, *b*; Ohba *et al.* 1994; Inoue *et al.* 1996; Mathonière *et al.* 1996; Iwamura

et al. 1998). What characterizes this field of research is its deeply multidisciplinary nature; it brings together synthetic organic, organometallic, and inorganic chemists along with theoreticians and physicists as well as material and life science people.

To a large extent, the field so far has been governed by the race toward high critical temperature, T_c, In that respect, T_c above room temperature is a must. This goal has been reached with a compound of formula $V^{II}_{0.42}V^{III}_{0.58}[Cr^{III}(CN)_6]_{0.86} \cdot 2.8H_2O$ (Ferlay *et al.* 1995). This compound belongs to the vast family of the Prussian blue-like phases with the general formula $A_k[B(CN)_6]_1 \cdot nH_2O$, where A is a high spin metal ion and B a low spin one. In contrast, not much effort has been devoted so far to the study of the phenomena arising from the magnetic anisotropy. The goal of this paper is to introduce this 'magnetic anisotropy' dimension in the field of molecule-based magnets. To do so we will focus on two aspects, namely, the design of a hard magnet through the incorporation of magnetically anisotropic spin carriers, and the determination of the magnetic phase diagrams of two strongly anisotropic ferromagnets synthesized from the $[Mo(CN)_7]^{4-}$ precursor.

2. Design of a very hard molecule-based magnet

In 1993, we reported on a compound containing three spin carriers, two metal ions and an organic radical, whose structure consisted of two interpenetrating quasi-perpendicular honeycomb-like networks (Stumpf *et al.* 1993, 1994*a*). This compound is a soft magnet, with a very small coercive field in the magnetically ordered state, below $T_c = 22.5$ K. The problem we were then faced with was the following. What chemical modifications should be made to introduce a significant memory effect? How to transform this compound to end up with a hard magnet? Here, we report on the solution we found. For that we compare two compounds, of formula

$$(Etrad)_2Mn_2[Cu(opba)]_3(DMSO)_{0.5} \cdot 0.25H_2O \qquad (\mathbf{1})$$

and

$$(Etrad)_2Co_2[Cu(opba)]_3(DMSO)_{1.5} \cdot 0.25H_2O \qquad (\mathbf{2}),$$

respectively. $Etrad^+$ is the radical cation shown below,

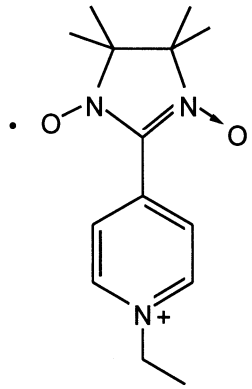

in which an unpaired electron is equally shared between the two nitroxide groups, opba is the ligand *ortho*-phenylenebis(oxamato), and S stands for solvent molecules. These compounds are isostructural. Their structure consists of two nearly perpendicular graphite-like networks with edge-sharing hexagons. The corners of each hexagon

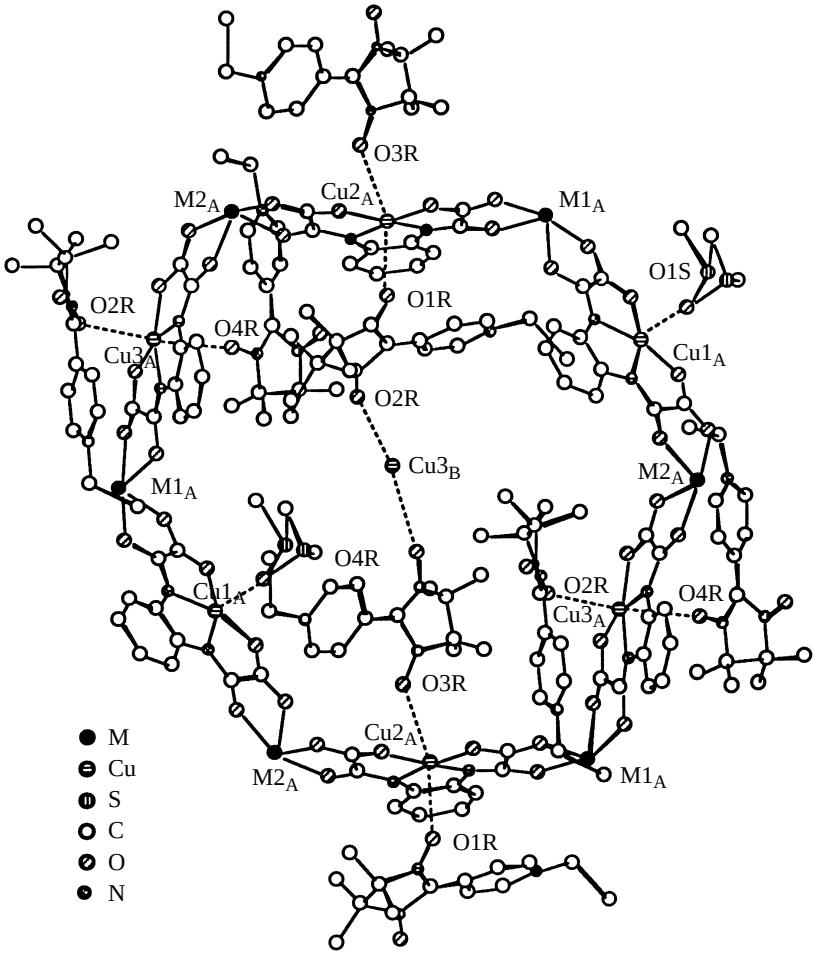

Figure 1. View of a hexagon in compounds **1** (M = Mn) and **2** (M = Co) along with the copper atom belonging to the nearly perpendicular network, located nearby the centre of the hexagon. This view also shows the presence of Cu^{II}–$Etrad^{+}$ chains connecting the two networks.

are occupied by M^{II} (Mn^{II} or Co^{II}) ions, and the middles of the edges by Cu^{II} ions. The two networks are interlocked, the centre of each hexagon being occupied by a Cu^{II} ion belonging to a nearly perpendicular hexagon. The compounds contain three kinds of spin carriers, M^{II} and Cu^{II} ions antiferromagnetically coupled through oxamato brigdes, and $Etrad^{+}$ cations, bridging the Cu^{II} ions through the nitronyl nitroxide groups, and forming Cu^{II}–$Etrad^{+}$ chains which further connect the two networks. Figure 1 shows the structure of a hexagon, and figure 2 the interlocking of the two graphite-like networks.

The magnetic properties of **1** and **2** were investigated in detail. Both compounds may be considered as ferrimagnets. The S_M (M = Mn or Co) spins align along the field direction, and the S_{Cu} and S_{Etrad} spins along the opposite direction. The temperature dependencies of the field-cooled magnetization (FCM) and the remnant magnetization (REM) are represented in figure 3. The critical temperatures were

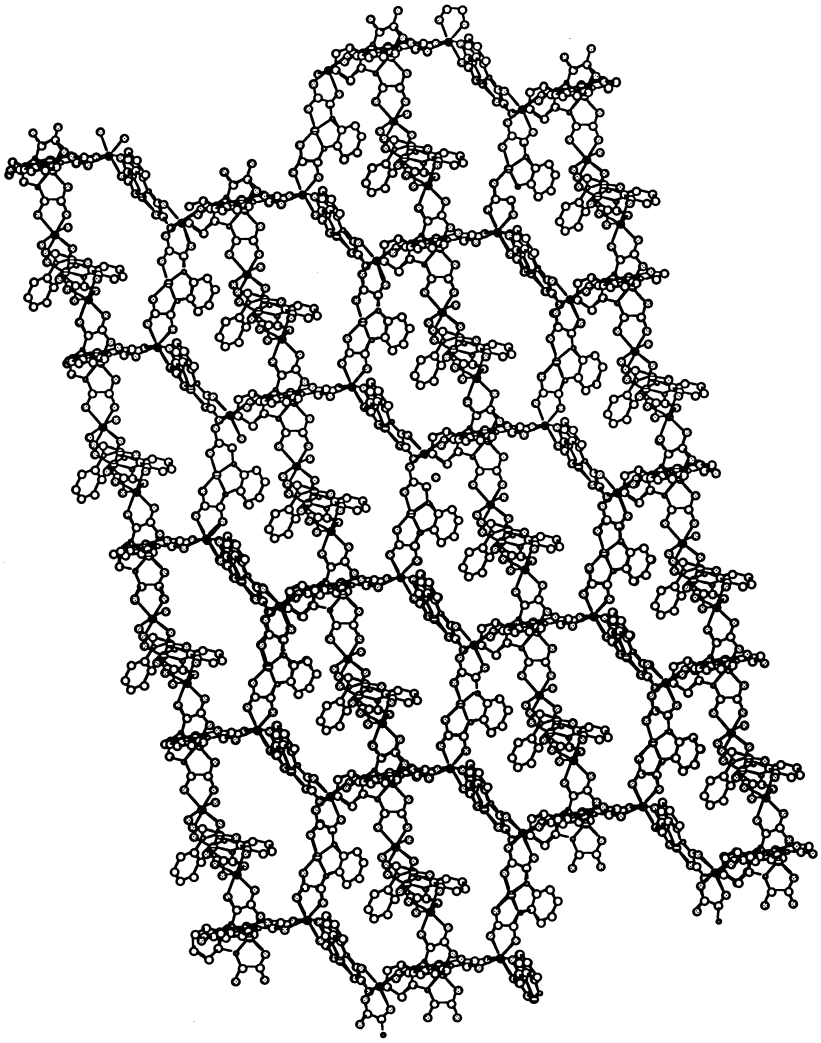

Figure 2. Interlocking of the two nearly perpendicular networks in compounds **1** and **2**.

determined as the extrema of the derivatives dFCM/dT, and found as $T_c = 22.8$ K for **1** and $T_c = 37$ K for **2**.

The main difference between the two compounds concerns the field dependencies of the magnetization in the magnetically ordered state, below T_c. **1** is a soft magnet. The field dependence of the magnetization at 5 K reveals a coercive field smaller than 10 Oe. In contrast, **2** is a very hard magnet. Figure 4 shows the hysteresis loop at 6 K for two samples consisting of crystals of different sizes. The black points were obtained with rather large crystals, and the coercive field is found as 8.5 kOe. The white points were obtained with crystals whose volume is roughly 50 times smaller, and the coercive field is of the order of 25 kOe.

The coercivity of a magnet depends on both chemical and structural factors (Stumpf *et al.* 1994*b*; Vaz *et al.* 1999). As far as the chemical factors are concerned,

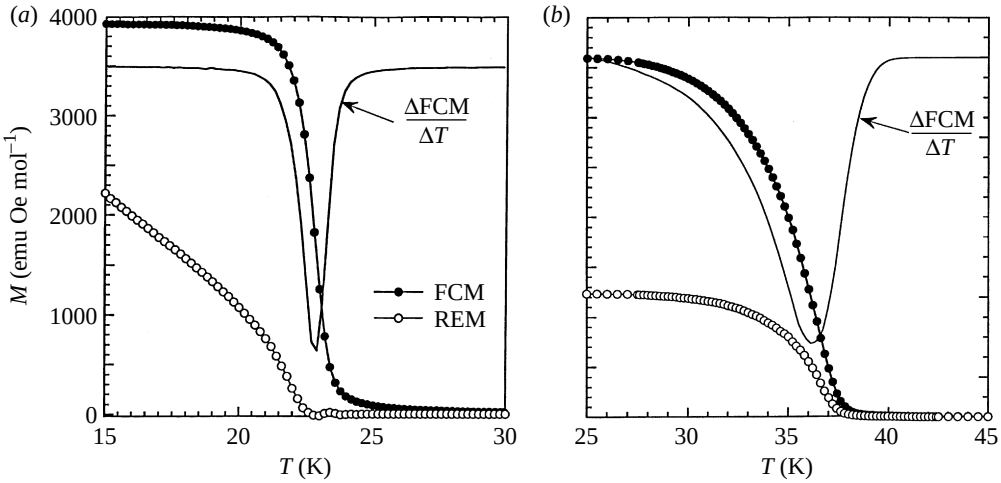

Figure 3. FCM and REM versus T curves for compound **1** (a) and **2** (b). The applied magnetic field is 20 Oe. The figure also shows the dFCM/dT derivatives.

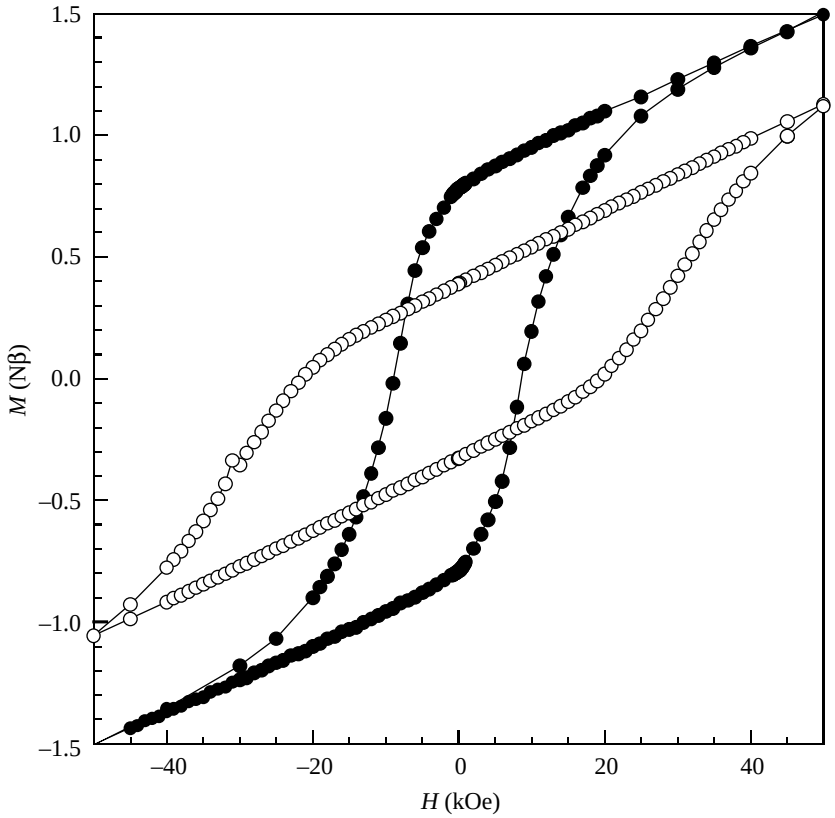

Figure 4. Field dependencies of the magnetization for two samples of compound **2**: (•) largest crystals; (○) smallest crystals.

the key role is played by the magnetic anisotropy of the spin carriers. The main structural factors are related to the size and shape of the particles. Here these two types of factors are illustrated. The high-spin Co^{II} ion in a distorted octahedral environment has a strong magnetic anisotropy, while the Mn^{II} ion in the same environment is almost isotropic. This chemical difference explains why compound **2** is much more coercive than compound **1**. The coercivity, however, is not an intrinsic property. It also depends on structural factors such as grain size and shape.

3. Magnetic phase diagrams for two cyano-bridged bimetallic ferromagnets synthesized from the $[Mo(CN)_7]^{4-}$ precursor

One of the appealing aspects of the magnetic studies dealing with Prussian blue phases (Babel 1986; Gadet *et al.* 1992; Mallah *et al.* 1993; Entley & Girolami 1994, 1995) resides in the fact that it is possible to predict the nature, and to estimate *a priori* the value of the critical temperature, using simple theoretical models based on the symmetry of the singly occupied orbitals (Kahn 1993). This is due to the fact that the symmetry of both the A and B metal sites is strictly octahedral, so that the e_g and t_{2g} orbitals do not mix. The design of the room temperature magnet mentioned in the introduction does not arise from serendipity, but was achieved in a rational way (Ferlay *et al.* 1995; Kahn 1995). The cubic symmetry of the Prussian blue phases, however, has a cost. These compounds are structurally, and hence magnetically, isotropic, and many interesting features associated with the structural and magnetic anisotropies cannot be observed. It may be noticed that nobody so far has succeeded in growing single crystals of Prussian blue phases suitable for detailed magnetic measurements. This situation is not too embarrassing as no anisotropy is expected, except perhaps a weak shape anisotropy for thin film samples. On the other hand, the thorough investigation of the properties of molecule-based magnets of low symmetry requires obviously to work with well-shaped single crystals.

Recently, we initiated a project concerning bimetallic compounds synthesized from the $[Mo(CN)_7]^{4-}$ precursor. The choice of this precursor was motivated by three reasons. (i) As for the Prussian blue phases, the presence of cyano ligands can lead to extended lattices. (ii) These networks should be of low symmetry; as a matter of fact, the heptacoordination of the precursor is not compatible with a cubic symmetry. (iii) In $KNa_2[Mo(CN)_7] \cdot 2H_2O$, the Mo^{III} ion is in a low-spin pentagonal bipyramid environment. The orbitally degenerate ground state, $^2E_1''$, is split into two Kramers doublets by the spin orbit coupling, and the ground Kramers doublet is strongly anisotropic (Rossman *et al.* 1973; Hursthouse *et al.* 1980; Young 1932).

(*a*) *The three-dimensional compound* $Mn_2(H_2O)_5Mo(CN)_7 \cdot 4H_2O$, *α phase* (**3**)

The slow diffusion of two aqueous solutions containing $K_4[Mo(CN)_7] \cdot 2H_2O$ and $[Mn(H_2O)_6](NO_3)_2$, respectively, affords two kinds of single crystals, with elongated plate (α phase) and prism (β phase) shapes (Larionova *et al.* 1998*a*, *b*). Here, we restrict ourselves to $Mn_2(H_2O)_5Mo(CN)_7 \cdot 4H_2O$, α phase (**3**). There is one molybdenum site along with two manganese sites, denoted as Mn1 and Mn2. The molybdenum atom is surrounded by seven –C–N–Mn linkages, four of them involving a Mn1 site and three of them a Mn2 site. The geometry may be described as a slightly distorted pentagonal bipyramid. Both Mn1 and Mn2 sites are in distorted octahedral

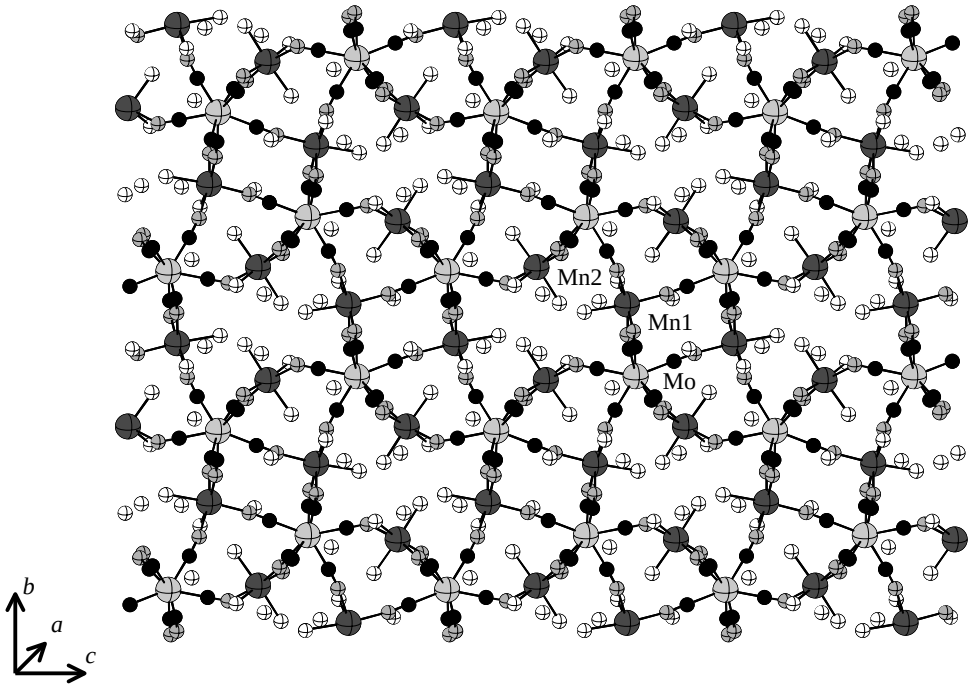

Figure 5. Structure of compound **3** viewed along the *a*-direction.

surroundings. Mn1 is surrounded by four –N–C–Mo linkages and two water molecules in *cis* conformation. Mn2 is surrounded by three –N–C–Mo linkages and three water molecules in a *mer* conformation. The three-dimensional organization for **3** may be described as follows. Edge-sharing lozenge motifs $(MoCNMn1NC)_2$ form bent ladders running along the *a*-direction. Each ladder is linked to four other ladders of the same kind along the [011] and [01$\bar{1}$] directions through cyano bridges. These ladders are further connected by the $Mn_2(CN)_3(H_2O)_3$ groups. Mn2 is linked to a Mo site of one of the ladders and to two Mo sites of the adjacent ladder. The structure as a whole viewed along the *a*-direction is represented in figure 5.

We first checked that in the three crystallographic planes *ab*, *bc* and *ac*, the extremes of the magnetization are obtained when the field is aligned along the *a*-, *b*- and c^*-axes. Therefore, these axes are the magnetic axes of the compound. It may be noticed that the twofold axis of the monoclinic lattice, *b*, was necessarily one of the magnetic axes (Wooster 1973). All the magnetic measurements were carried out on single crystals with the external field successively applied along these three axes. We first measured the temperature dependencies of the magnetization, M, under a field of 5 Oe. The three curves are shown in figure 6. They reveal that the material is anisotropic, the magnetization along the easy magnetization axis, *b*, being about twice as large as along the *a*-axis. Moreover, these curves exhibit a break with an inflexion point at $T_{1c} = 50.5$ K, along with another anomaly, more visible along the *a*-axis, at $T_{2c} = 43$ K.

The most accurate technique to determine transition temperatures is the measure of the heat capacity as a function of temperature. In the present case, the heat capacity curve shows a lambda peak at 50.5 K, but nothing is detected at 43 K.

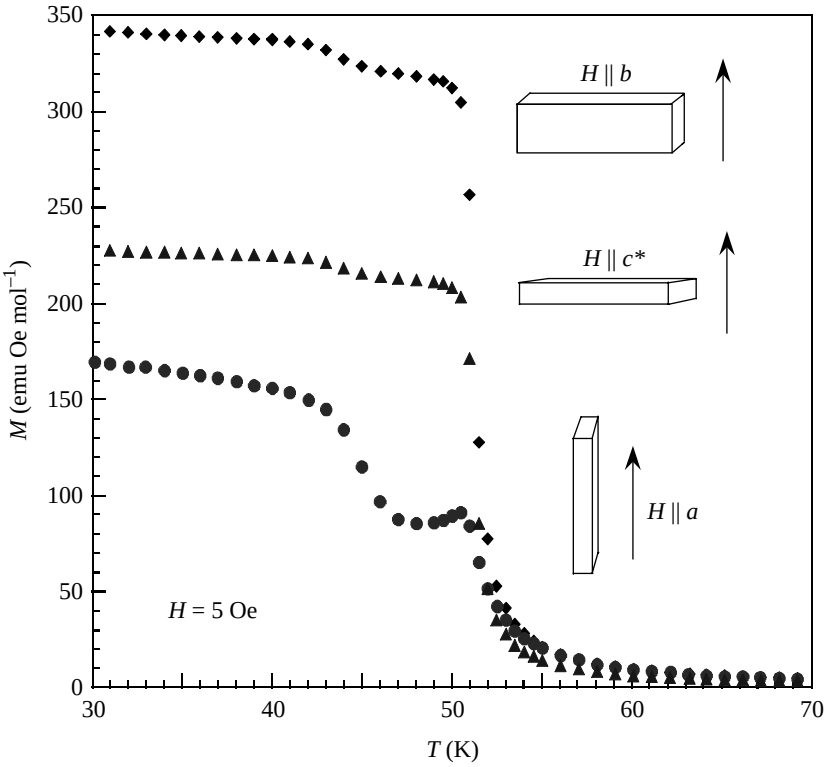

Figure 6. Temperature dependencies of the magnetization along the *a*-, *b*- and c^*-directions, using an external field of 5 Oe, for compound **3**.

In order to obtain more insights on the magnetic anomaly detected at 43 K, visible essentially along the *a*-direction, we measured the magnetization along this direction with an external field varying from 1 up to 100 Oe. The results are displayed in figure 7. T_{2c} is shifted toward higher temperatures as the magnetic field increases, and eventually, for a field of *ca.* 100 Oe, merges with the transition at 50.5 K. For each field, T_{2c} was determined as the inflexion point of the $M = f(T)$ curve.

We then measured the field dependencies of the magnetization at 5 K along the *a*-, *b*- and c^*-directions (see figure 8). The curves are strictly identical when increasing and decreasing the field; the compound exhibits no coercivity. Along the easy magnetization direction, *b*, the saturation is reached with *ca.* 1 kOe. The saturation magnetization is found to be equal to 11 Nβ. This value corresponds to what is expected for one $S_{\mathrm{Mo}} = 1/2$ and two $S_{\mathrm{Mn}} = 5/2$ local spins aligned along this direction. The interaction between adjacent $\mathrm{Mo^{III}}$ and $\mathrm{Mn^{II}}$ ions is ferromagnetic. Along the c^*-direction, the magnetization increases progressively when applying the field, and even at 50 kOe the saturation is not totally reached. Along the *a*-direction, the *M* versus *H* curve is peculiar; it shows an inflexion point for a critical field, H_{c}, of about 2.2 kOe. We are faced with a field-induced spin reorientation phenomenon (Salgueiro da Siva *et al.* 1995; Garcia-Landa *et al.* 1996; Mendoza & Shaheen 1996; Cao *et al.* 1997; Kou *et al.* 1997).

Let us examine in more detail what happens when applying the field along the *a*-axis. In zero field, the resulting moment of 11 Nβ is essentially aligned along *b*. When

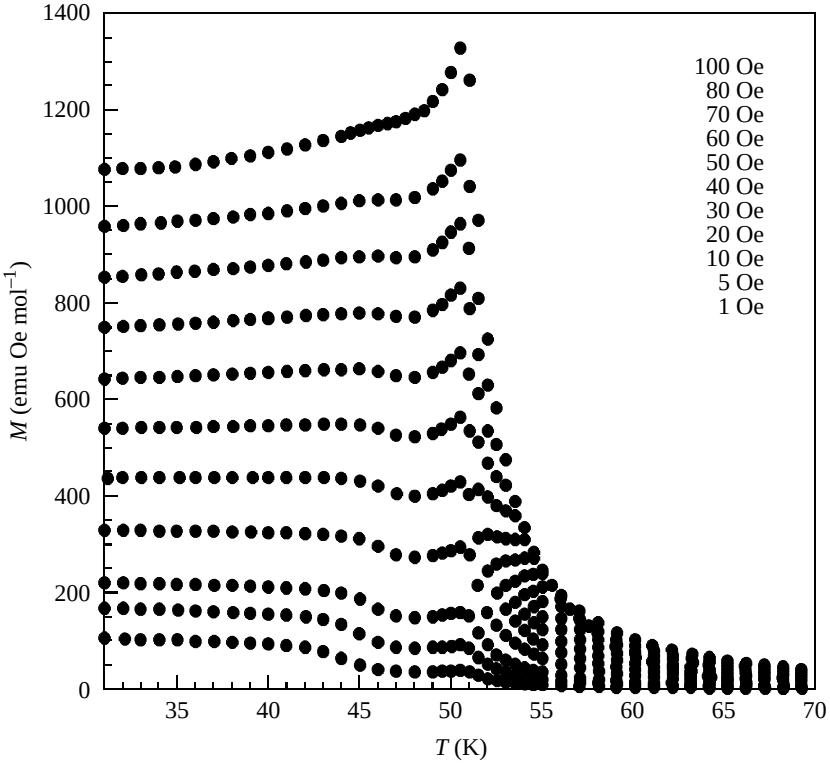

Figure 7. Temperature dependencies of the magnetization along the *a*-direction, using different values of the external field, for compound **3**.

applying the field, first this moment hardly rotates from b to a, then for a critical value of the field the rotation becomes much easier. Finally, for a saturation value of the field, H_{sat}, the moment is aligned along a. The spin reorientation is a nonlinear phenomenon. It is difficult to unhook the moment from the b-axis. When the field is large enough this unhooking is realized, and then a weak increase of the field induces a strong rotation until the moment is collinear with a. To determine the H_{c} and H_{sat} versus T curves, we measured the field dependence of the magnetization along a every 5 K in the 5–51 K range. The critical field at each temperature was determined as the field for which the $\mathrm{d}M/\mathrm{d}H$ derivative is maximum. The saturation field at each temperature was determined as the weakest field for which the saturation is reached.

The temperature dependencies of H_{c} and H_{sat} for a field applied along the a-axis are used to determine the magnetic phase diagram of the compound. This diagram, shown in figure 9, presents four domains. Domain I is the paramagnetic domain in which the spins are either randomly oriented, or aligned along the field direction. Domains II and III are ferromagnetic domains in which the spins are essentially aligned along the b-direction. Domain III is limited to the 43–51 K temperature range and the 0–100 Oe field range. Domain IV, finally, is limited by the $H_{\mathrm{c}} = f(T)$ and $H_{\mathrm{sat}} = f(T)$ curves, and corresponds to a mixed domain in which the spins may rotate easily from the b- to the a-direction. It is worth mentioning that the

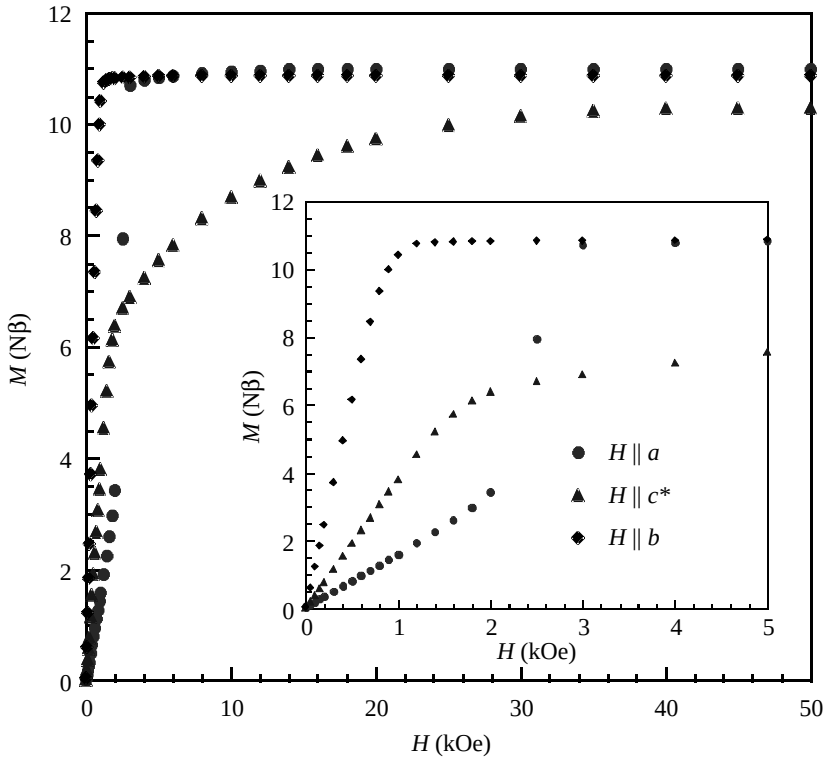

Figure 8. Field dependencies of the magnetization at 5 K along the *a*-, *b*- and c^*-directions for compound **3**.

boundary between domains II and IV corresponds to a first-order transition, while that between domains I and IV corresponds to a second-order transition.

The magnetic data suggest that the main difference between domains II and III concerns the component of the resulting moment along *a*. Assuming that the magnetic symmetry of the low-temperature domain II is lower than that of the high-temperature domain III, we may assume that domain III is a perfectly ferromagnetic domain with the magnetic moments aligned along *b* in zero field, and that a small canting occurs as *T* is lowered below 43 K, with a weak component of the resulting moment along *a*. Alternatively, the two domains might be weakly canted, with a component of the moment along *a*, the degree of canting being slightly more pronounced in domain II.

(*b*) *The two-dimensional compound* $K_2Mn_3(H_2O)_6[Mo(CN)_7]_2 \cdot 6H_2O$ (**4**)

When the slow diffusion between aqueous solutions containing $K_4[Mo(CN)_7]\cdot 2H_2O$ and $[Mn(H_2O)_6](NO_3)_2$, respectively, takes place in the presence of an excess of K^+ ions, a two-dimensional compound of formula $K_2Mn_3(H_2O)_6[Mo(CN)_7]_2 \cdot 6H_2O$ is obtained (Larionova *et al.* 1999). The structure again contains a unique molybdenum site along with two manganese sites, denoted as Mn1 and Mn2. The molybdenum atom is surrounded by six –C–N–Mn linkages and a terminal –C–N ligand. The geometry may be described as a strongly distorted pentagonal bipyramid, and both the

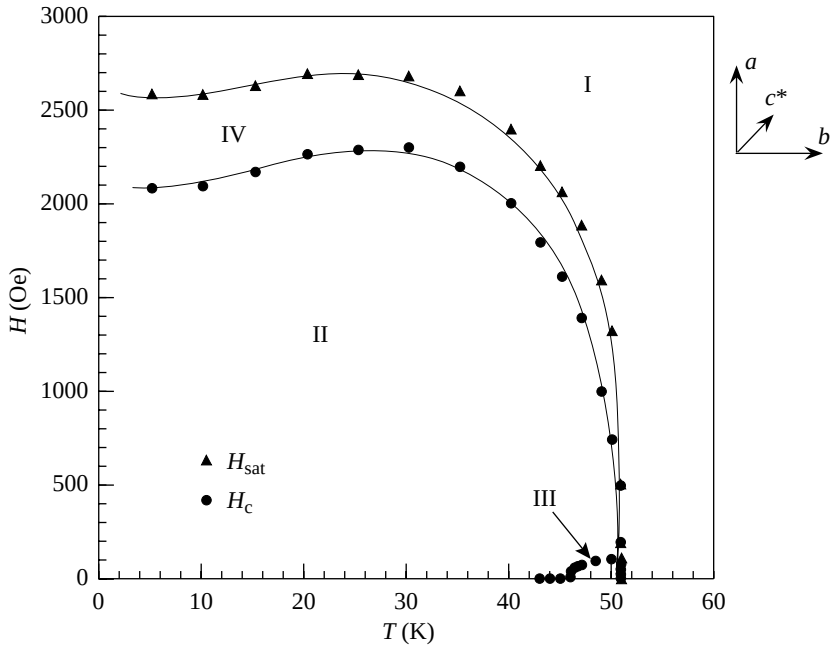

Figure 9. Magnetic phase diagram for compound **3**; the full lines are just eye-guides.

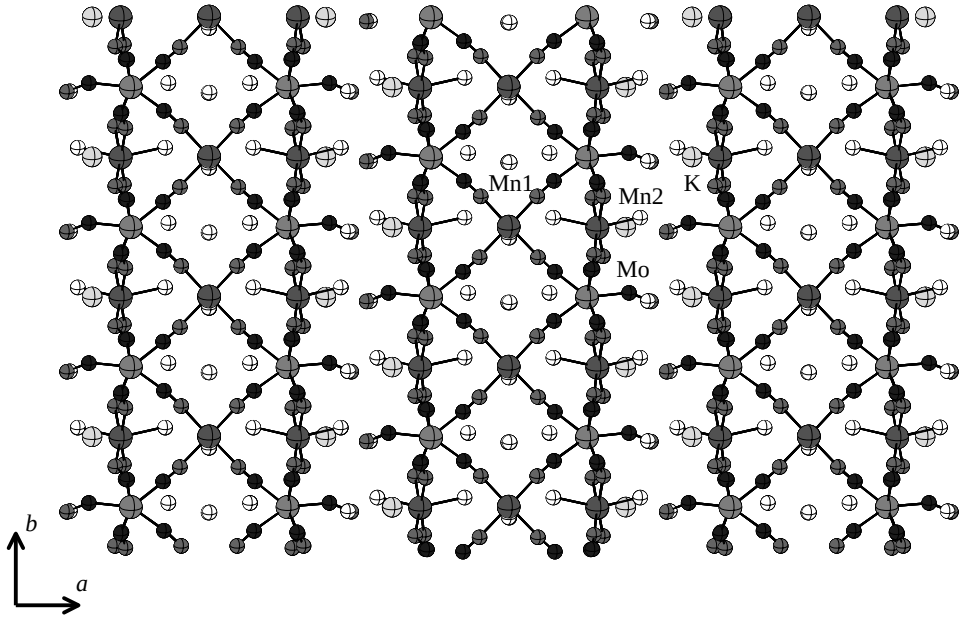

Figure 10. Structure of the compound **4** in the *ab*-plane.

Mo–C–N and C-N–Mn bridging angles deviate significantly from 180°. Both the Mn1 and Mn2 sites are surrounded by four –N–C–Mo linkages and two water molecules in *trans* conformation. The two-dimensional structure is made of anionic double-sheet layers parallel to the *bc*-plane, and K^+ and non-coordinated water molecules situ-

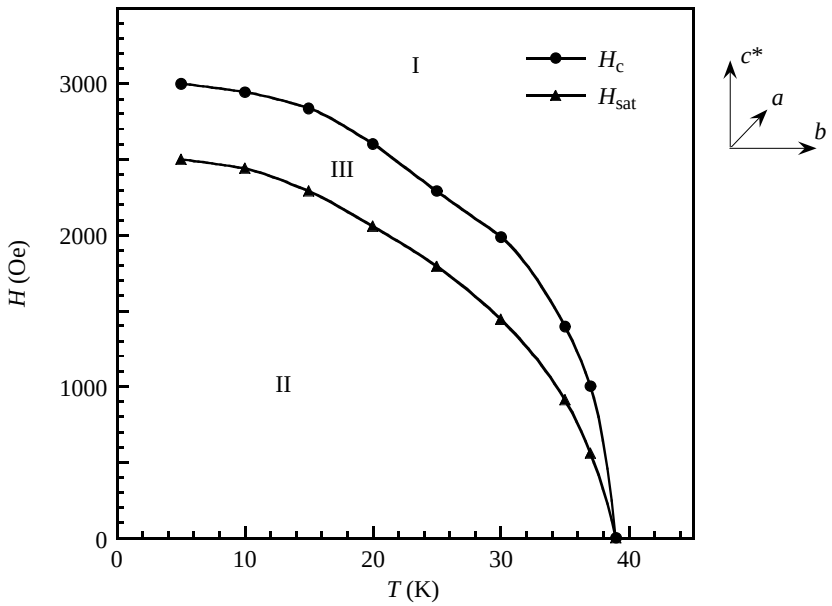

Figure 11. Magnetic phase diagram for the compound **4**; the full lines are just eye-guides.

ated between the layers, as shown in figure 10. Each sheet is a kind of grid in the *bc*-plane made of edge-sharing lozenges $[MoCNMn_2NC]_2$. Two parallel sheets of a layer are further connected by $Mn1(CN)_4(H_2O)_2$ units situated between the sheets. The thickness of a double-sheet layer is 8.042 Å, and that of the gap between two layers is 7.263 Å.

We first checked that a, b and c^* were the magnetic axes of the compound, b being the easy magnetization axis, then we studied the temperature and field dependencies of the magnetization along the three axes. No hysteresis was observed along a and b, while a narrow hysteresis, of about 125 Oe, was observed along c^* at 5 K. These measurements revealed that the compound exhibits a long-range ferromagnetic ordering at $T_c = 39$ K, and that below T_c a field-induced spin reorientation occurs along the c^*-axis. We determined the critical and saturation fields every 5 K below T_c when applying the field along c^*. The H_c and H_{sat} versus T curves shown in figure 11 define the magnetic phase diagram for the compound when the magnetic field is applied along c^*. This diagram is simpler than that of figure 9. It presents only three domains. Domain I corresponds to the paramagnetic, or saturated paramagnetic domain. Domain II corresponds to the ferromagnetically ordered domain in which the spins are essentially aligned along the b-axis. Domain III, finally, is a spin-reorientation domain in which the spins rotate from the b- to the c^*-direction as the field increases from H_c to H_{sat}.

So far, we have only spoken of magnetic measurements recorded in the DC mode, i.e. with a static external field. Additional information can be obtained by working in the AC mode (Palacio *et al.* 1989). We report here on two experiments of this kind. First, we measured the temperature dependencies of the in-phase, χ'_{AC}, and out-of-phase, χ''_{AC}, magnetic susceptibilities under a zero static field. Along the three directions, the in-phase responses exhibit a break at $T_c = 39$ K. The χ'_{AC} values along the b-axis below T_c are much higher than along the other two directions. The

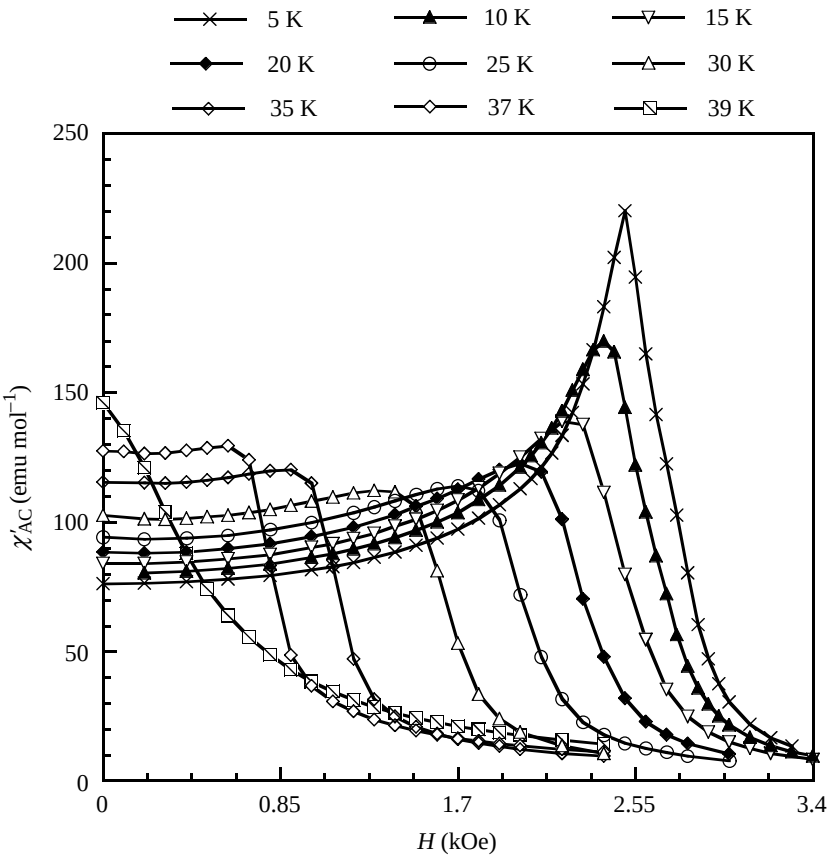

Figure 12. Field dependencies of the in-phase AC susceptibilities at different temperatures along the c^*-axis for the compound **4**.

out-of-phase response along the b-axis is zero down to 39 K, then presents an abrupt break as T is lowered below this temperature, and reaches a maximum around 34 K. Along the other two directions, χ''_{AC} is negligibly weak down to 2 K.

When the field is applied along the easy magnetization axis, b, both the displacement of the domain walls and the rotation of the magnetic moments contribute to the AC magnetic response. On the other hand, when the field is applied along a hard magnetization axis, only the rotation of the magnetic moments contributes to the AC response (Kou *et al.* 1996). In the present case, the very high response along b as compared with the responses along a and c^* indicates that the domain walls move very easily, which is in line with the quasi-absence of hysteresis in the $M = f(H)$ curves.

The second experiment consisted of measuring the field dependence of χ'_{AC} along the c^*-axis every 5 K in the magnetically ordered phase. The results are displayed in figure 12. At each temperature χ'_{AC} first increases as the field increases, reaches a maximum, then tends to zero at high field. The maximum of χ'_{AC} determines the critical field, H_c, and the extreme of the derivative $d\chi'_{AC}/dH$ determines the saturation field, H_{sat}. The $H_c = f(T)$ and $H_{sat} = f(T)$ curves deduced from this experiment are strictly similar to those shown in figure 11.

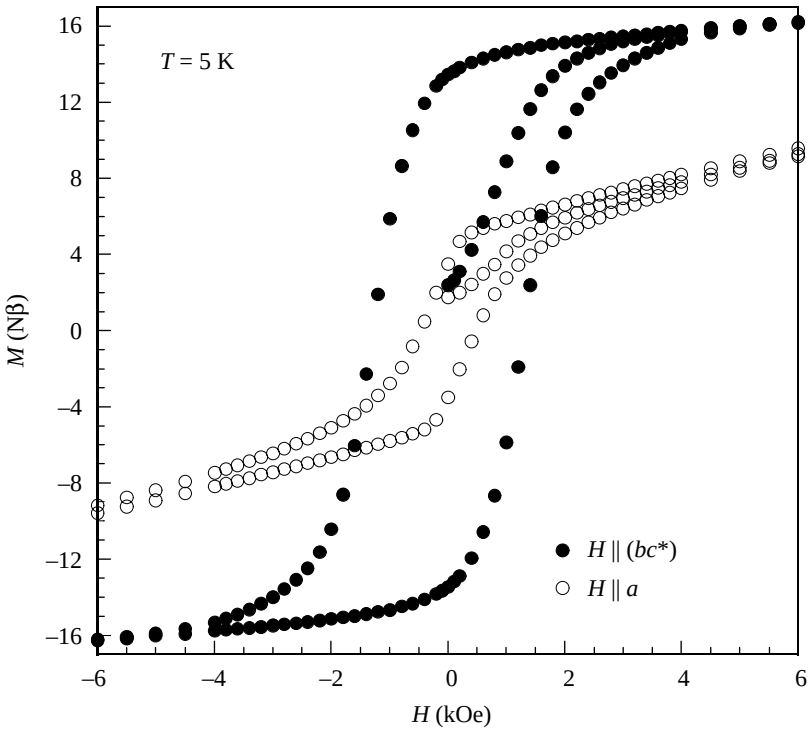

Figure 13. Hysteresis loops in the bc^*-plane and along the a-axis at 10 K for a partly dehydrated crystal of compound **4**.

(*c*) *Modification of the magnetic properties through partial dehydration*

The magnetic properties of $K_2Mn_3(H_2O)_6[Mo(CN)_7]_2 \cdot 6H_2O$ can be dramatically modified through partial dehydration. When the non-coordinated water molecules of a single crystal are released under vacuum, the external shape of the crystal is not modified. Magnetic measurements suggest that the crystallographic directions are retained. We then investigated the temperature dependencies of the magnetization along these directions. The $M = f(T)$ curves along b and c^* are not distinguishable. After dehydration, the bc-plane may be considered as an easy magnetization plane, even in low field. The spin reorientation is suppressed. Both in the bc-plane and perpendicular to this plane, the magnetization shows a break at $T_c = 72$ K, while the critical temperature for the non-dehydrated compound is 39 K. We measured the field dependencies of the magnetization at 10 K both in the bc^*-plane and along the a-direction. The results are displayed in figure 13. In the easy magnetization plane, the saturation value of 17 Nβ corresponding to the parallel alignment of all the spins is obtained under *ca.* 5.0 kOe. On the other hand, along the a-axis, the saturation is not reached yet under 50 kOe. Magnetic hystereses are observed along both directions, with coercive fields of 1.3 kOe in the bc-plane, and 0.55 kOe along a.

We can notice here that the Prussian blue phases are also hydrated. It would be interesting to see whether their partial dehydration also modifies their magnetic properties.

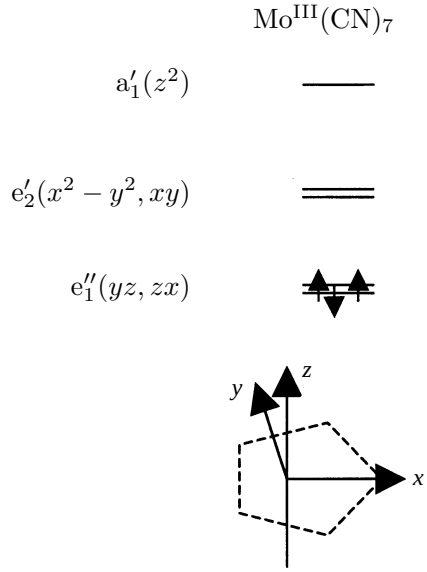

Scheme 1.

(*d*) *Why is the* Mo^{III}–C–N–Mn^{II} *interaction ferromagnetic?*

One of the striking features concerning the compounds described in this article is the ferromagnetic nature of the interaction between low-spin Mo^{III} and high-spin Mn^{II} ions through the cyano bridge. For several decades, quite a few studies have been devoted to the microscopic mechanisms of the interaction between spin carriers, more particularly to those of the mechanisms favouring a parallel alignment of the electron spins (Kahn 1993; Kollmar & Kahn 1993). Three situations have been found to stabilize the parallel spin state, namely the following. (i) *The strict orthogonality of the magnetic orbitals.* Such a situation is achieved when all the singly occupied orbitals centred on a spin carrier (also called magnetic orbitals) are orthogonal (i.e. give a zero overlap integral) with all the singly occupied orbitals centred on the adjacent spin carrier. This situation of strict orthogonality of the magnetic orbitals is certainly the most efficient way to achieve a ferromagnetic interaction. (ii) *The electron transfer from a singly occupied orbital on a site toward an empty orbital on an adjacent site, or from a doubly occupied orbital on a site toward a singly occupied orbital on an adjacent site.* This mechanism is probably less efficient than the previous one, and more difficult to control. (iii) *The interaction between a zone of negative spin density on a fragment and a zone of positive spin density on an adjacent fragment.* This mechanism, first suggested in the context of assemblies of organic radicals (McConnell 1963), may apply for transition metal species as well.

We carefully examined the relevance of each of these mechanisms in the case of Mo^{III}–C–N–Mn^{II}. The strict orthogonality of the magnetic orbitals is not realized, and the absorption spectra of the compounds synthesized from the $[Mo(CN)_7]^{4-}$ precursor do no reveal any metal–metal charge transfer band of relatively low energy. Therefore, we are wondering whether the ferromagnetic interaction could arise from a close contact between negative and positive spin density zones.

The orbital energy diagram for low-spin Mo^{III} in pentagonal bipyramid symmetry (D_{5h}) is represented in scheme 1.

At the self-consistent field (SCF) approximation, the $e'_2(x^2 - y^2, xy)$ and $a'_1(z^2)$ orbitals with a predominant 4d character are empty. It follows that at this approximation level, there is no spin density along both equatorial and axial Mo–C–N directions. It is now well established that such a view is oversimplified. The $^2E''_1$ SCF ground state may couple with SCF excited states of the same symmetry in which electrons have been promoted from the doubly occupied and bonding e'_2 and a'_1 orbitals with a predominant cyano character to the empty and antibonding e'_2 and a'_1 orbitals with a predominant metal character. This configuration interaction gives rise to a negative spin density in the σ orbitals of the cyano ligands, along the Mo–C–N directions. This spin polarization effect has been experimentally observed in the hexacyanometallates involving 3d ions, such as $[Cr(CN)_6]^{3-}$ and $[Fe(CN)_6]^{3-}$, from polarized neutron diffraction experiments (Figgis *et al.* 1987, 1993). The crucial point is that the stronger (i.e. the more covalent) the M—(CN) bond is, the more pronounced the spin polarization. Owing to the diffuseness of the 4d orbitals compared with the 3d orbitals, the Mo^{III}—(CN) bond is significantly stronger than the Cr^{III}—(CN) or Fe^{III}—(CN) bond. It follows that the negative spin density along the Mo–C–N directions of the $Mo(CN)_7$ fragment might be particularly important. If it was so, the interaction between this negative spin density with a σ character and the σ singly occupied orbitals of Mn^{II} might favour the parallel alignment of the S_{Mo} and S_{Mn} spins.

(*e*) *What is the origin of the anisotropy?*

Let us list the various factors affording magnetic anisotropy. We begin with the two local factors: the anisotropy of the $\boldsymbol{g}$ tensors and the zero-field splitting of the local spin states for the magnetic ions with a local spin higher than 1/2. In addition, there are several many-body (or collective) factors. These are (i) the anisotropic interactions, resulting from the synergistic effect of the local spin-orbit coupling for an ion and the interaction between the excited states of this ion and the ground state of the adjacent ion; (ii) the antisymmetric interaction whose origin is similar to that of anisotropic interaction, but in addition requires a low lattice symmetry; (iii) the dipolar interactions which may become important for lattices of low symmetry, and/or for high local spins (for instance, $S_{Mn} = 5/2$); (iv) the shape anisotropy, finally, depending on the shape and size of the single crystals or particles used for the magnetic measurements (Bencini & Gatteschi 1989). Applying an external field H along the easy magnetization axis results in an internal field H_i related to H through

$$H_i = H - NM,$$

where N is the demagnetizing factor depending on the shape anisotropy, and NM the demagnetizing field. The field dependencies of M shown in figure 8 are not corrected of the demagnetizing field.

Except when all the local spins are 1/2, the local zero-field splittings are usually more important than the anisotropic interactions. As for the antisymmetric interaction, it leads to the spin canting, which may superimpose to both an antiferromagnetic or a ferromagnetic state. In this latter case, it gives rise to the phenomenon of weak ferromagnetism.

What are the relevant factors in the case of the compounds described in this article? Mn^{II} in octahedral surroundings has a $^6A_1$ ground state, with a very weak zero-field splitting. On the other hand, the $\boldsymbol{g}$ tensor for the $[Mo^{III}(CN)_7]$ chromophore is expected to be strongly anisotropic (Hursthouse *et al.* 1980). In other respects, the lattice symmetries are very low, even for the three-dimensional compounds. It follows that the two main anisotropy factors are the anisotropy of the $\boldsymbol{g}$ tensor for the $[Mo^{III}(CN)_7]$ chromophore along with the dipolar interactions. The spin reorientation might be due to a competition between these two factors. In zero (or low) external field, the ferromagnetically coupled local spins tend to align along the direction of the Mo–C–N–Mn–C–N infinite linkages (for instance, the *b*-axis for $Mn_2(H_2O)_5Mo(CN)_7\cdot 4H_2O$, α phase), which minimizes the dipolar energy. When the magnetic field reaches a certain value, the $\boldsymbol{g}$ anisotropy for Mo^{III} favours the spin alignment along another direction.

4. Conclusion

In this paper, we have explored two facets of the magnetic anisotropy in the field of molecule-based magnets. First, we have been concerned by the coercivity. The possibility to design molecule-based magnets displaying wide magnetic hysteresis loops was not obvious, at least for us. Actually, some time ago, we thought that the softness of the molecular state would prevent us from synthesizing very coercive magnets. We were not right; there is no contradiction between soft lattices and hard magnets. The key factor of the coercivity for compound **2** is the presence of the very anisotropic Co^{2+} spin carrier. This factor, however, is not the only one. The Co^{2+}-containing two-dimensional magnets of formula $cat_2Co_2[Cu(opba)]_3\cdot S$ display coercive fields at 6 K weaker than 5 kOe (Stumpf *et al.* 1994*b*). The three-dimensional character of **2** resulting from the interlocking of two quasi-perpendicular graphite-like networks also contributes to the coercivity.

The second part of this paper deals with the peculiar magnetic phase diagrams arising from the low symmetry. In the field of molecule-based magnets, this low symmetry may lead to very interesting physical phenomena. Of course, the thorough investigation of these phenomena and their correct interpretation require work on single crystals, which is time-consuming and sometimes not trivial. However, accepting to do so may be very rewarding. To the best of our knowledge, the spin reorientation phenomenon had only been found so far for ferromagnetic intermetallic compounds, and not for insulating ferromagnets. In other respects, the magnetic phase diagrams of figures 9 and 11 are the very first for magnetic materials synthesized from molecular precursors.

This work was partly funded by the TMR Research Network ERBFMRXCT980181 of the European Union, entitled ‘Molecular Magnetism: from Materials toward Devices’.

References

Babel, D. 1986 *Comments Inorg. Chem.* **5**, 285.
Bencini, A. & Gatteschi, D. 1989 *EPR of exchange coupled systems*. Springer.
Broderick, W. E., Thompson, J. A., Day, E. P. & Hoffman, B. M. 1990 *Science* **249**, 410.
Caneschi, A., Gatteschi, D., Sessoli, R. & Rey, P. 1989 *Acc. Chem. Res.* **22**, 392.
Cao, G., McCall, S. & Crow, J. E. 1997 *Phys. Rev.* B **55**, R672.

Chiarelli, R., Nowak, M. A., Rassat, A. & Tholence, J.-L. 1993 *Nature* **363**, 147.
Decurtins, S., Schmalle, H. W., Oswald, H. R., Linden, A., Ensling, J., Gütlich, P. & Hauser, A. 1994*a* *Inorg. Chim. Acta* **216**, 65.
Descurtins, S., Schmalle, H. W., Schneuwly, P., Ensling, J. & Gütlich, P. 1994*b* *J. Am. Chem. Soc.* **116**, 9521.
Entley, W. R. & Girolami, G. S. 1994 *Inorg. Chem.* **33**, 5165.
Entley, W. R. & Girolami, G. S. 1995 *Science* **268**, 397.
Ferlay, S., Mallah, T., Ouahès, R., Veillet, P. & Verdaguer, M. 1995 *Nature* **378**, 701.
Figgis, B. N., Forsyth, J. B. & Reynolds, P. A. 1987 *Inorg. Chem.* **26**, 101.
Figgis, B. N., Kucharski, E. S. & Vrtis, M. 1993 *J. Am. Chem. Soc.* **115**, 176.
Gadet, V., Mallah, T., Castro, I. & Verdaguer, M. 1992 *J. Am. Chem. Soc.* **114**, 9213.
Garcia-Landa, B., Tomey, E., Fruchart, D., Gignoux, D. & Skolozdra, R. 1996 *J. Magn. Magn. Mater.* **157–158**, 21.
Gatteschi, D. 1994 *Adv. Mater.* **6**, 635.
Hursthouse, M. B., Maijk, K. M. A., Soares, A. M., Gibson, J. F. & Griffith, W. P. 1980 *Inorg. Chim. Acta* **45**, L81.
Inoue, K. & Iwamura, H. 1994 *J. Am. Chem. Soc.* **116**, 3173.
Inoue, K., Hayamizu, T., Iwamura, H., Hashizume, D. & Ohashi, Y. 1996 *J. Am. Chem. Soc.* **118**, 1803.
Iwamura, H., Inoue, K. & Koga, N. 1998 *New J. Chem.* **10**, 201.
Kahn, O. 1993 *Molecular magnetism.* New York: VCH.
Kahn, O. 1995 *Nature* **378**, 667.
Kahn, O., Pei, Y., Verdaguer, M., Renard, J.-P. & Sletten, J. 1988 *J. Am. Chem. Soc.* **110**, 782.
Kollmar, C. & Kahn, O. 1993 *Acc. Chem. Res.* **26**, 259.
Kou, X. C., Grössinger, R., Hischer, G. & Kirchmayr, H. R. 1996 *Phys. Rev.* B **54**, 6421.
Kou, X. C., Dahlgren, M., Grössinger, R. & Wiesinger, G. 1997 *J. Appl. Phys.* **81**, 4428.
Larionova, J., Sanchiz, J., Golhen, S., Ouahab, L. & Kahn, O. 1998*a* *Chem. Commun.*, p. 953.
Larionova, J., Clérac, R., Sanchiz, J., Kahn, O., Golhen, S. & Ouahab, L. 1998*b* *J. Am. Chem. Soc.* **120**, 13 088.
Larionova, J., Kahn, O., Gohlen, S., Ouahab, L. & Clérac, R. 1999 *J. Am. Chem. Soc.* **121**, 3349.
McConnell, H. M. 1963 *J. Chem. Phys.* **39**, 1910.
Mallah, T., Thiebaut, S., Verdaguer, M. & Veillet, P. 1993 *Science* **262**, 1554.
Mathonière, C., Nuttall, C. J., Carling, S. & Day, P. 1996 *Inorg. Chem.* **35**, 1201.
Mendoza, W. A. & Shaheen, S. A. 1996 *J. Appl. Phys.* **79**, 6327.
Miller, J. S. & Epstein, A. J. 1994 *Angew. Chem. Int. Ed.* **33**, 385.
Miller, J. S., Calabrese, J. C., Epstein, A. J., Bigelow, R. W., Zang, J. H. & Reiff, W. M. 1986 *J. Chem. Soc. Chem. Commun.*, p. 1026.
Miller, J. S., Calabrese, J. C., Rommelman, H., Chittipedi, S. R., Zang, J. H., Reiff, W. M. & Epstein, A. J. 1987 *J. Am. Chem. Soc.* **109**, 769.
Nakazawa, Y., Tamura, M., Shirakawa, N., Shiomi, D., Takahashi, M., Kinoshita, M. & Ishikawa, M. 1992 *Phys. Rev.* B **46**, 8906.
Ohba, M., Maruono, N. & Okawa, H. 1994 *J. Am. Chem. Soc.* **116**, 11 566.
Palacio, F., Lazaro, F. J. & Duyneveldt, A. J. 1989 *Mol. Crys. Liq. Cryst.* **176**, 289.
Pei, Y., Verdaguer, M., Kahn, O., Sletten, J. & Renard, J.-P. 1986 *J. Am. Chem. Soc.* **108**, 428.
Rossman, G. R., Tsay, F. D. & Gray, H. B. 1973 *Inorg. Chem.* **12**, 824.
Salgueiro da Siva, M. A., Moreira, J. M., Mendes, J. A., Amaral, V. S., Sousa, J. B. & Palmer, S. B. 1995 *J. Phys.: Condens. Mater.* **7**, 9853.
Stumpf, H. O., Ouahab, L., Pei, Y., Grandjean, D. & Kahn, O. 1993 *Science* **261**, 447.

Stumpf, H. O., Ouahab, L., Pei, Y., Bergerat, P. & Kahn, O. 1994*a* *J. Am. Chem. Soc.* **116**, 3866.

Stumpf, H. O., Pei, Y., Michaut, C., Kahn, O., Renard, J. P. & Ouahab, L. 1994*b* *Chem. Mater.* **6**, 257.

Tamaki, H., Zhong, Z. J., Matsumoto, N., Kida, S., Koikawa, S., Achiwa, S., Hashimoto, Y. & Okawa, H. 1992 *J. Am. Chem. Soc.* **114**, 6974.

Vaz, M. G. F., Pinheiro, L. M. M., Stumpf, H. O., Alcântara, A. F. C., Gohlen, S., Ouahab, L., Cador, O., Mathonière, C. & Kahn, O. 1999 *Chem. Eur. J.* **5**, 1486.

Wooster, W. A. 1973 *Tensor and group theory for the physical properties of crystals*. Oxford: Clarendon Press.

Yee, G. T., Manriquez, J. M., Dixon, D. A., McLean, R. S., Groski, D. M., Flippen, R. B., Narayan, K. S., Epstein, A. J. & Miller, J. S. 1991 *Adv. Mater.* **3**, 309.

Young, R. C. 1932 *J. Am. Chem. Soc.* **54**, 1402.

PHILOSOPHICAL TRANSACTIONS OF THE ROYAL SOCIETY A MATHEMATICAL, PHYSICAL & ENGINEERING SCIENCES

PHILOSOPHICAL TRANSACTIONS OF THE ROYAL SOCIETY A MATHEMATICAL, PHYSICAL & ENGINEERING SCIENCES